KfK 3988 B
Dezember 1985

A Gas-Silicon Telescope for Medium-heavy Ion Detection

T. Kozik, J. Buschmann, M. Neudold
Institut für Kernphysik

Kernforschungszentrum Karlsruhe

KERNFORSCHUNGSZENTRUM KARLSRUHE

Institut für Kernphysik

KfK 3988 B

A GAS-SILICON TELESCOPE FOR MEDIUM-HEAVY ION DETECTION

T. Kozik*, J. Buschmann, M. Neudold

* Permanent address:
Institute of Physics, Jagellonian University, Cracow, Poland

Kernforschungszentrum Karlsruhe GmbH, Karlsruhe

Kernforschungszentrum Karlsruhe GmbH
Postfach 3640, 7500 Karlsruhe 1

ISSN 0303-4003

Zusammenfassung

EIN GAS-SILIZIUM-TELESKOP ZUR ERFASSUNG MITTELSCHWERER IONEN

Zur Identifizierung energiereicher mittelschwerer Ionen ($Z < 12$) wurde ein ΔE-E-Teleskop gebaut, das aus einer Frisch-Gitter-Ionisationskammer zur Messung des spezifischen Energieverlustes und aus einem Si-Oberflächensperrschichtzähler zur Messung der Restenergie besteht. Die theoretischen Gesichtspunkte, die für die Energie- und die Zeitauflösung des Gasdetektors maßgeblich sind, werden diskutiert. Das Gasversorgungssystem, dessen Ventile mittels eines Betriebsartenschalters zentral gesteuert werden, und 2 verschiedene Versionen der Koinzidenzelektronik werden beschrieben. Am Beispiel eines 2-dimensionalen E-ΔE-Spekrums wird gezeigt, daß die erreichte Z-Auflösung der mit dieser Technik zu erwartenden Güte entspricht.

Summary

A ΔE-E telescope for the identification of medium-heavy ions is presented. The specific energy loss is measured with a gas ionization chamber, and the residual energy is determined with a silicon surface barrier detector. The main features of the collecting electrical field and the timing properties of the device are discussed under theoretical aspects. The gas supply system, its electronic control unit, and the operating procedures are described. Two different versions of the coincidence electronics are shown. The experimental performance of the gas-silicon telescope is demonstrated and is found to be close to the best Z-resolution which can be obtained with this technique.

Contents

1. Introduction

In typical ΔE-E telescopes for particle detection either a very thin surface barrier counter or a thin scintillator or an ionization chamber is used for measurement of the specific energy loss /1/ - /3/. For detection of light particles, $Z \leq 3$, or of heavier ions with sufficiently high energies detectors of the first or second type are suited. On the other hand, numerous advantages, like variable thickness of the ΔE layer, high homogeneity, and a good resistance to radiation damage make the gas ΔE ionization chamber one of the most commonly used detectors in heavy ion experiments.

However, there are also disadvantages, namely much poorer timing characteristics of the gas chamber compared with silicon or scintillator detectors, the necessity of an additional gas equipment, and a smaller signal to noise ratio due to the small thickness of the gas medium and due to the higher energy required to generate an ion-electron pair (e.g. 30 eV in a (90 % Ar + 10 % CH_4) mixture compared with 3.6 eV in Si or 2.9 eV in Ge).

2. Description of the Telescope

In Fig. 1 the cross section of the gas-silicon telescope is shown. The tracks of the ions begin at the entrance window (40-60 $\mu g/cm^2$ Mylar foil) which is provided at the right hand side of part (2), pass through the gas medium and are stopped by the 4 mm thick surface barrier

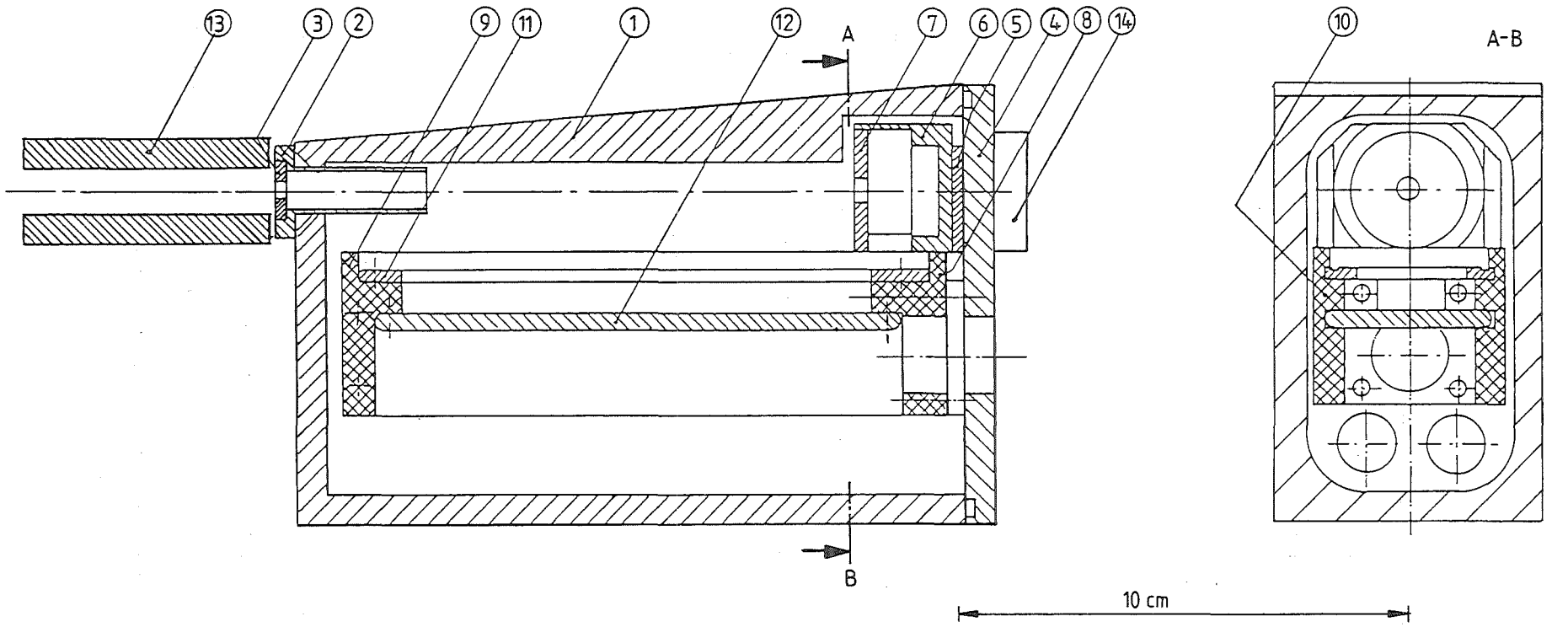

(1) container
(2) entrance tube
(3) diaphragm
(4) back cover
(5) Si-detector mounting
(6) Si-detector housing
(7) diaphragm
(8) support for Frisch grid and anode
(9) end piece
(10) Plexiglas shields
(11) frame for the Frisch grid
(12) anode
(13) repeller for δ electrons
(14) cooling plate for the Si-detector

Fig. 1. Horizontal cross section of the gas-silicon telescope.

detector (ORTEC 24-331A) installed in part (6). The magnetic yoke (13), which consists of two permanet magnets, serves to remove any external electrons that could otherwise enter the gas counter. The electrons produced by ionization drift through the Frisch grid /4/ and are collected by the anode, whereas the positive ions are neutralized after they have arrived at the container wall, which acts as the cathode. The container (1) is fabricated from a solid aluminium block and closed with the brass plate (4) from the rear side. The oblique outer profile of the housing, similar to the design described in Ref. /5/, permits a close approach to the beam, typically 2.5^{o} at 280 mm distance between the target and the front side of the telescope. All necessary electrical and gas-feed throughputs, the semiconductor detector housing (6) with the collimator (7), the external cooling plate (14), which allows to cool the Si-detector down to -40 ^{o}C, and the grid-anode assembly are attached to the rear flange (4). The grid frame (11) and the anode (12) are fixed by the properly shaped isolating end-pieces (8), (9) and shielded on both sides by Plexiglas walls (10). This precaution is necessary to prevent electrons from entering the region near the edges of the electrodes where the electrical field is very high and charge avalanche multiplication is very likely to occur. Due to the rigid design of the grid-anode assembly possible resonant vibrations resulting in microfonic noise are minimized. Figure 2 shows a photograph of the layout of the telescope interior.

The grid was wound in two different manners, one with 40 µm diameter wire (Isabellenhütte Heusler GmbH, 80 % Ni + 20 % Cr) and 0.4 mm spacing, and the other with 20 µm diameter wire and 0.3 mm spacing.

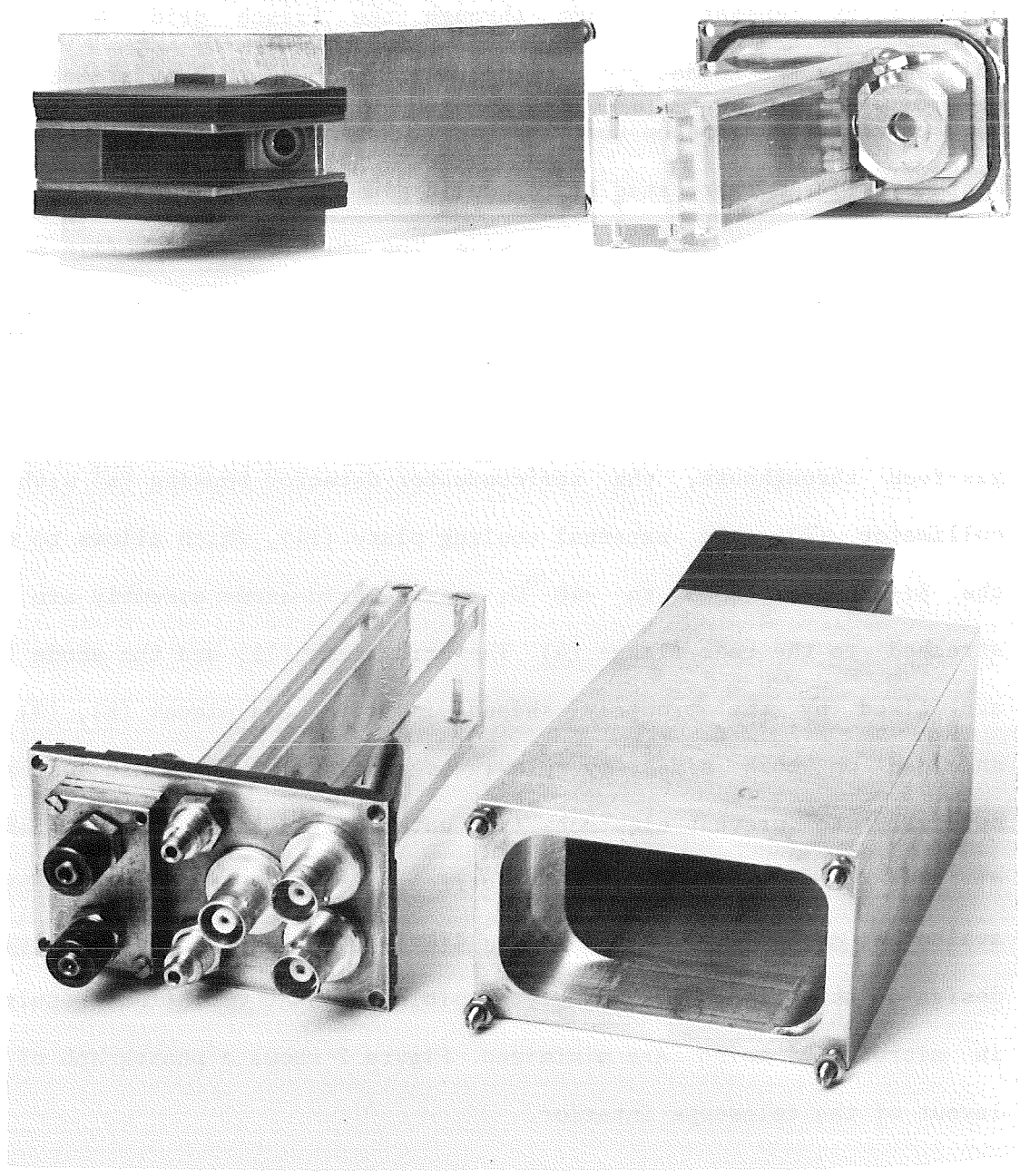

Fig. 2: General view of the container and the interior of the gas-silicon telescope.

For preparation of the grids a special winder was designed which is shown in Fig. 3. The wire distance is given by the lead of threaded bars (9) fixed in the corners of parts (5). After winding is completed the wires are cemented on the front surfaces of part (9). Then the wires are cut along the groves formed by parts (5) with part (4) with a razor blade so that two identical grids are produced. Then these grids are transferred to the grid frames (part (11) of Fig. 1). While the wires are soldered on one side of the grid frame they are cemented on the other side using cold-hardening glue in order to avoid thermal delatation.

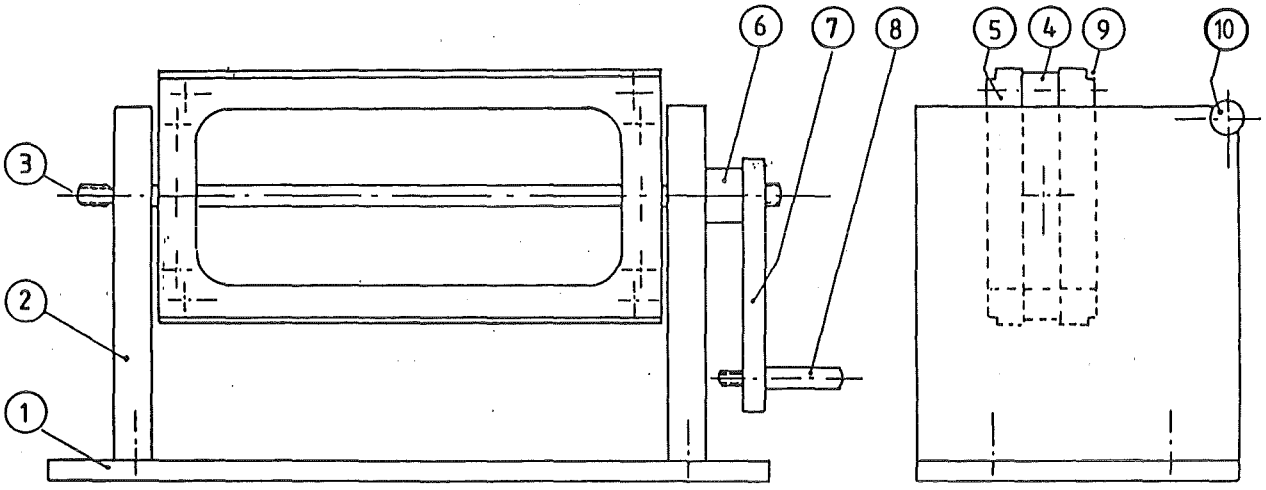

(1) base plate
(2) side walls
(3) axle
(4) supporting frame
(5) winding frame
(6) spacer
(7) crank
(8) handle grip
(9) threaded bars
(10) guiding bar

Fig. 3: Grid winder.

3. Design Requirements

The following special problems have to be considered in ΔE gas detector design:

* minimizing the amount of not utilized energy deposited in the gas;
* broadening the electron cloud and path length variation due to diffusion; focusing the electrons to the Frisch grid;
* recombination; gas contamination by desorption of impurities from the construction materials; operating voltages;
* effects of the space charge due to the slowly moving positive ions;
* transparency and efficiency of the Frisch grid;
* timing properties.

Some of the problems above are interdependent. Most of them are caused by the electrical field geometry, which will, consequently, be discussed in more detail.

The mobility of electrons, which amounts to approximately 4 - 6 cm/μs in the (Ar-CH_4) mixture at 50 mbar /6/, differs from that of positive ions by a factor of about 10^3. The positive ions produce a space charge which drifts slowly towards the cathode. This space charge reduces significantly the effective field for the electrons. Therefore, the collection times and their fluctuations are much greater than they would be otherwise. Even if the screening effect

of the positive space charge is ignored, the rate of change of the induced charge (note that the cathode-anode assembly constitutes a parallel plate capacitor) and, after pulse shaping, the amplitute of the ΔE signals are position dependent.

In order to make the ΔE signals position independent, the anode is screened from the positive space charge by the Frisch grid. Obviously, one has to find a compromise between the efficiency and transparency of such a wire grid. Our Frisch grid was dimensioned according to the following optimum conditions /7/:

$$\frac{|\vec{E}_{cg}|}{|\vec{E}_{ga}|} \geq \frac{1+\rho}{1-\rho} \qquad ; \qquad \rho = \frac{2 \cdot \pi \cdot r}{d}$$

$$\frac{V_{ga}}{V_{cg}} \geq \frac{s_{cg} \cdot (1+\rho) + 2 \cdot 1 \cdot \rho}{s_{ga} \cdot (1-\rho) - 2 \cdot 1 \cdot \rho} \qquad ; \qquad 1 = \frac{d}{2 \cdot \pi} \cdot \left(\frac{\rho^2}{4} - \ln(\rho)\right) \tag{1}$$

where E_{cg} and E_{ga} are the electric fields in the cathode-grid and the grid-anode space, respectively, r is the radius of the grid wire and d the wire distance, V_{cg} and V_{ga} are the voltages between the cathode/grid and the grid/anode, respectively, and s_{cg} and s_{ga} are the cathode-grid and the grid-anode separations. The wire spacing d was optimized by minimizing the inefficiency /7/, /8/ of the grid given by

$$\frac{d}{2 \cdot \pi \cdot s_{cg}} \cdot \ln\left(\frac{d}{2 \cdot \pi \cdot r}\right) \tag{2}$$

according to the wire diameters available. E_{cg} was imposed so that

the drift velocity of electrons in (90 % Ar + 10 % CH_4) gas at the operating pressure of 65 mbar approaches the maximum value (see also discussion of E/p in Chap. 5). The s_{cg} parameter is limited by the dimension of the overlapping Si-detector housing as well as by the requirement of Eq. (2) and was chosen as small as possible. Then the remaining parameters s_{ga} and V_{ga} are obtained by solving Eqs. (1).

4. Description of the Gas Supply System

The gas supply was controlled by a module whose front panel is shown in Fig. 4. The gas control system had originally been used for the acceptance detector of the Karlsruhe Magnetic Spectrograph "Little John" /9/ but was adapted to run the ΔE gas detector in a 130 cm diameter scattering chamber with its own pumping system. The valves V3A and V3B with their switches are not considered in this case. V21, V23, and V25 were not installed. In Tab. 1 the settings of the different valves are listed.

Tab. 1: Functional logic of the gas control
(0 = closed / off; 1 = open / on)

Mode of Operation	V21	V22	V23	V24	V25	V26	R11
"Evakuieren"	0	1	0	0	0	1	1
"Betrieb mit Gas"	1	0	0	0	0	1	1
"Betrieb ohne Gas"	0	0	0	0	0	1	1
"Belüften"	0	1	0	1	0	0	0

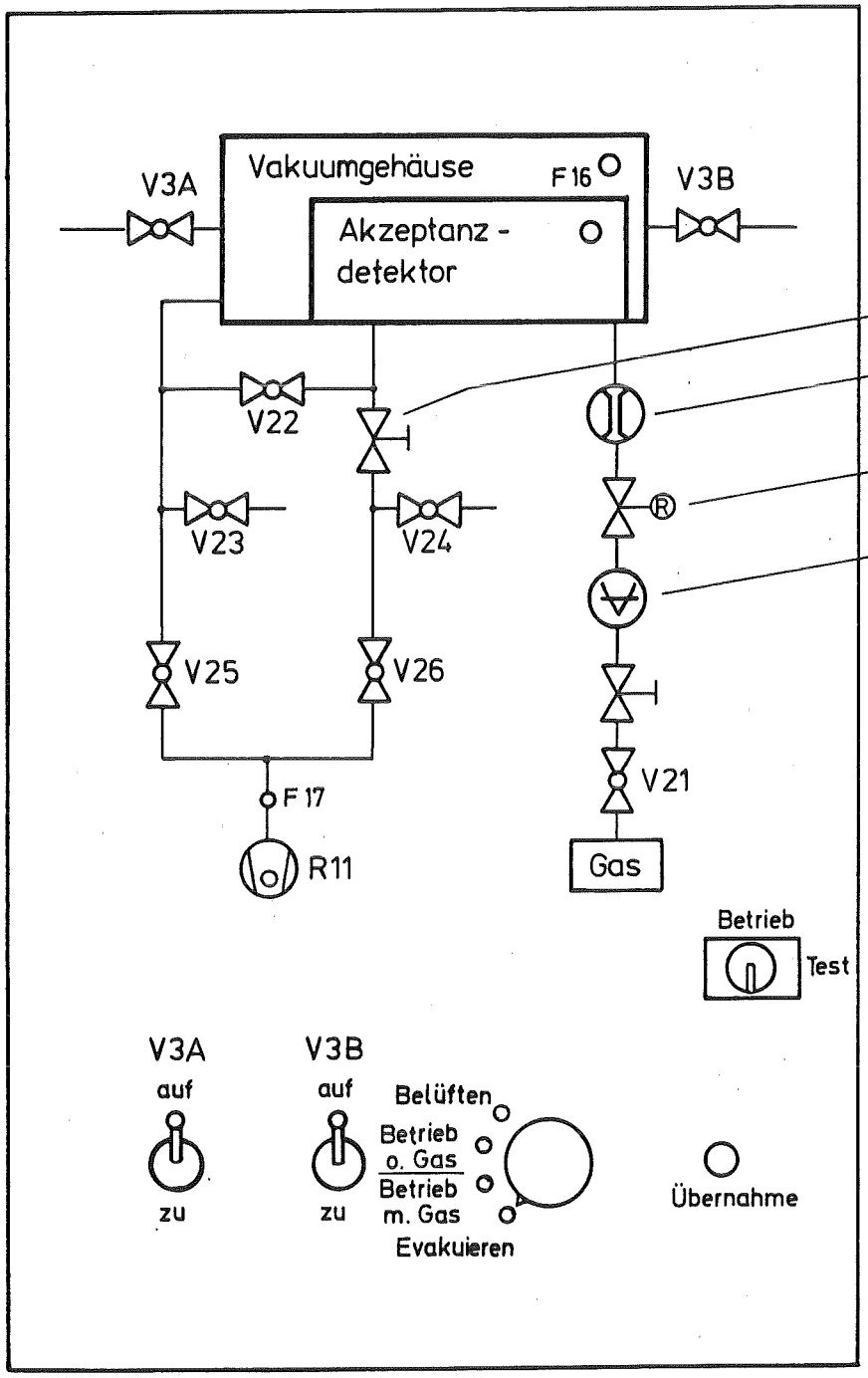

A: Manually operated needle valve
B: Flowmeter
C: Pressure control unit (Vacuum General 80-1)
D: Absolute pressure meter (Balzers APG 010)

Fig. 4: Front panel of the gas control unit.

The electric circuit diagram of the gas control unit is shown in Fig. 5. The logic is burned in the EPROM 74S188.

Evacuation and flooding procedures of the big scattering chamber which are not handled by the control unit but must be done manually still require some attention. This is a list of proven operational sequences which guarantee the survival of the fragile Mylar window of the gas detector:

Evacuation of the scattering chamber under the following initial conditions:
Both the scattering chamber and the gas detector installed are at atmospheric pressure; both the rotary pump and the turbomolecular pump of the scattering chamber are flooded; both the valves above the rotating pump and above the turbomolecular pump are open; the pressure downstream of the pressure attenuator is set to zero:

1) Close the scattering chamber.
2) Select the "Evakuieren" operation mode and push the "Übernahme" button.
3) Switch on the rotary pump; close, if open, the flooding valve on top of the scattering chamber.
4) When the vacuum gauge (D) shows less than about 1 mbar, select "Betrieb mit Gas", push the "Übernahme" button, and switch on the turbomolecular pump.
5) Raise to about 0.4 bar the pressure downstream of the pressure attenuator.
6) Set the desired operating gas pressure at the "Vacuum General" control unit (C) by means of the multiturn potentiometer;

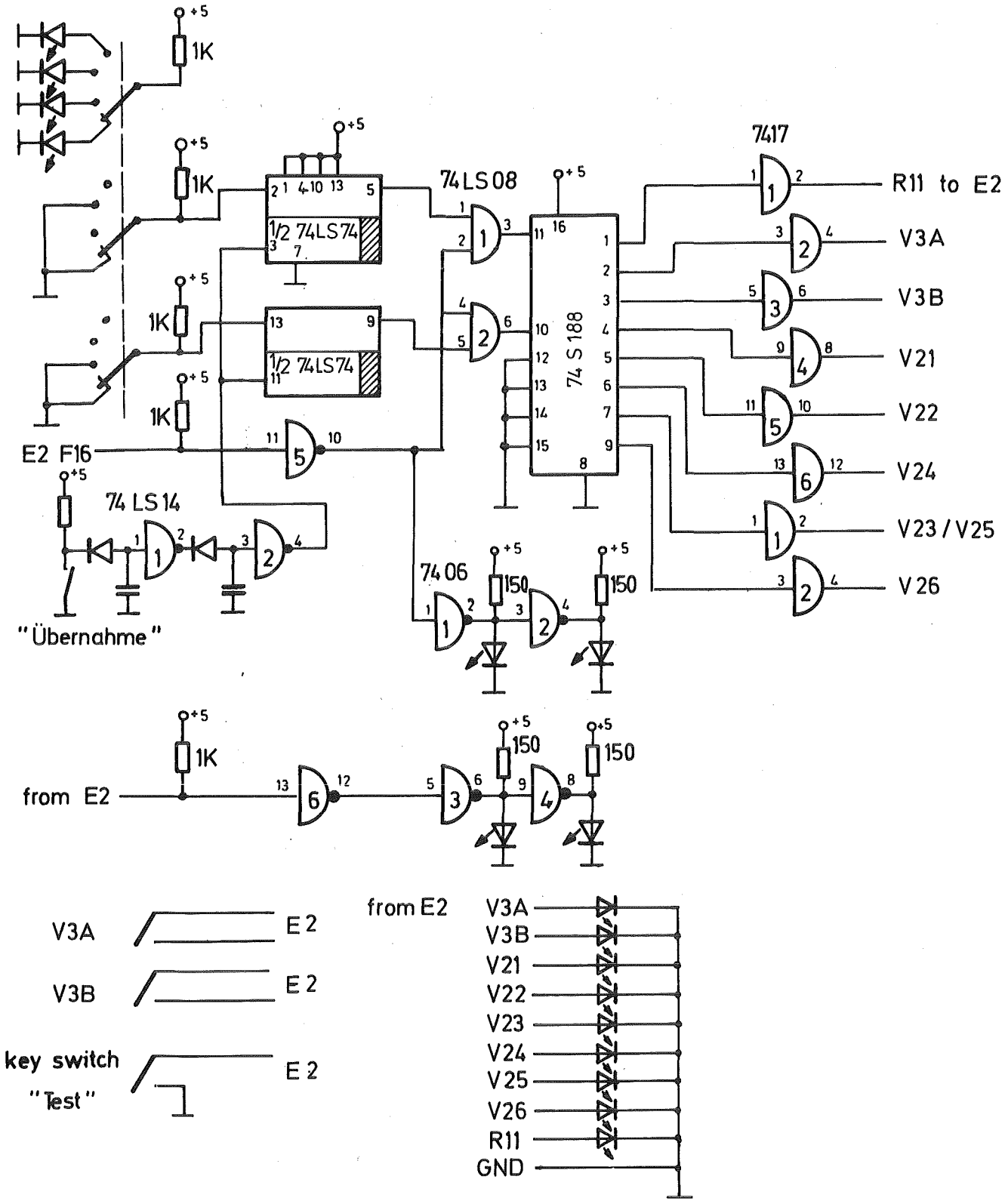

Fig. 5: Electronic scheme of the gas control unit. The output lines are connected with power amplifiers installed in a separate module.

7) Adjust the gas flow by the needle valve (A).

Flooding the scattering chamber together with the gas detector

under the following initial conditions:

The operating voltages of the telescope are off, and the valve, which separates the scattering chamber from the beam line, is closed:

1) Reduce to zero the pressure downstream of the pressure attenuator.
2) Close the needle valve (A).
3) Select the "Belüften" operation mode and push the "Übernahme" button.
4) Close the valve above the turbomolecular pump.
5) Open slowly the flooding valve on top of the scattering chamber (less than 5 mbar/s).
6) Open the chamber.
7) Execute all operations mentioned above in order to be ready for re-evacuation.

If the electronic gas control system is not available, the gas supply can be operated manually. For this application, the scheme of the gas system is shown in Fig. 6, and the settings of the valves are listed below.

	V1	V2	V3	V4	V6	V7
Evacuate / Flood	0	0	1	1	1	0
Set / Check Flow	1	1	1	0	0	0
Operate	1	0	0	1	0	0

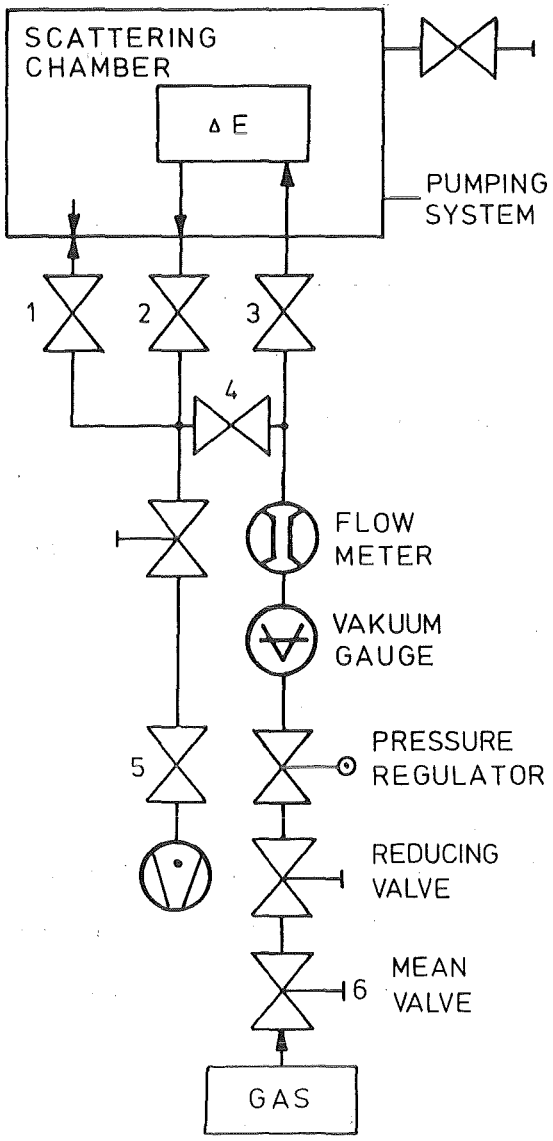

Fig. 6: Gas supply system for manual operation.

5. Electronics

The electronics required for running the telescope is composed of standard research equipment. The schemes (Fig. 7) contain the analog branches which provide pulses for the list mode acquisition, and the fast branches which elaborate coincidence signals.

To calculate the coincidence time needed one has to take into account the statistical variation in the time of electron drifting due to multiple scattering, Δt_1, and, in addition, the electron drift time dependence Δt_2 on the position of the particle path in the gas chamber. The average radial distance of electron diffusion while drifting over a distance L in a uniform electrical field E is given by /10/

$$\bar{r} = 0.17 \cdot \sqrt{\frac{L \cdot \eta}{E}} \qquad (3)$$

where η is the ratio of agitational energy of the free electrons to that of gas molecules. Taking $\eta = 250$ for pure argon and $\eta = 8.6$ for methane at 1 (V/cm)/mbar /10/, one gets $\bar{r}$-values less than 0.8 cm corresponding to Δt_1 = 50-200 ns due to diffusion parallel to the electric field. The variation of the particle path to the Frisch grid gives Δt_2 values on the order of some 100 ns. Actually, the coincidence time should be two times longer for safety reasons than that required by the theoretical estimate, that is at least 0.5 µs.

With this time resolution either a slow coincidence unit (e.g. ORTEC

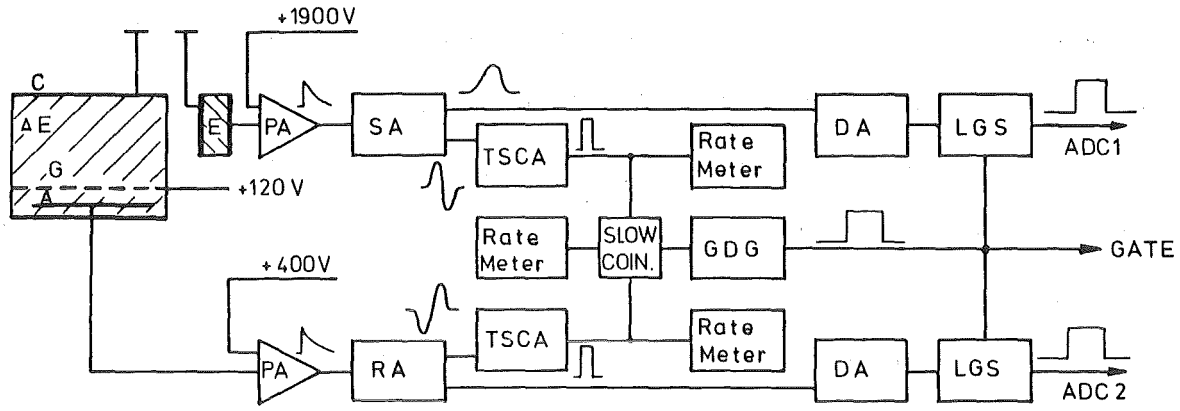

PA = preamplifier, e.g. Canberra 2005, ORTEC 142AH
SA = spectroscopy amplifier, e.g. ORTEC 572
RA = research amplifier, e.g. ORTEC 450
TSCA = timing single channel amplifier, e.g. ORTEC 553
GDG = gate and delay generator, e.g. ORTEC 416A
DA = delay amplifier, e.G. ORTEC 427A
LGS = linear gate and stretcher, e.g. ORTEC 542

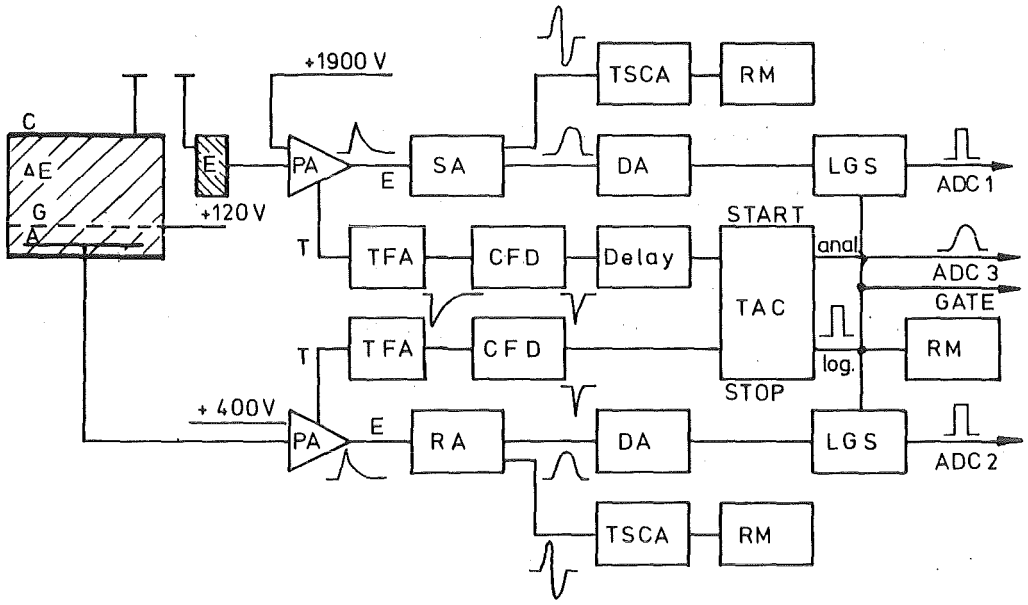

TFA = timing filter amplifier, e.g. ORTEC 474
CDF = constant fraction discriminator, e.g. ORTEC 473A
RM = ratemeter

Fig. 7: Alternative electronic schemes.
Upper part: Use of slow coincidence unit.
Lower part: Use of time-to-amplitude converter.

Universal Coincidence 418A) or a time-to-amplitude converter (TAC, e.g. ORTEC 467) can be used. The electronic setup with the slow coincidence unit is shown in the upper part of Fig. 7. Due to its simplicity and satisfactory performance this setup is commonly preferred. The electronic unit, which delivers timing signals, should work in the "constant fraction" mode (e.g. timing single channal analyzer ORTEC Model 551 / 553) rather than with the conventional leading-edge discrimination. Otherwise, the rise time resolution is degraded.

In case of high counting rates and strict timing requirements a TAC module together with a constant fraction discriminator can be used, as shown in the lower part of Fig. 7. The apparent advantage of this configuration is that the performance of the gas-silicon telescope can be permanently controlled by inspection af the TAC output spectrum.

The mean diffusion radius estimated from Eq. (3) gives also a rough value of the lateral width of the electron cloud at the grid plane, at least in a uniform electrical field. The actual lateral grid width (inner dimension of the frame) of the present design is 2.4 cm which seems to be sufficient, especially if the focusing property of the electrical field is taken into account.

6. Performance in the Experiment

The voltages applied to the gas detector were adjusted experimentally. Optimum values were found to be dependant above all on the dimensions of the Frisch grid. In some particular cases, where the voltage line contributed significantly to the net noise of the chamber, the anode was grounded with other potentials shifted accordingly.

The performance of the detector is sensitive to the operating voltages since the ratio of the electrical field to gas pressure, E/p, affects the drift velocity of the electrons which has a maximum, e.g. at 0.75 (V/cm)/mbar in pure methane and at 7.5 (V/cm)/mbar in isobutane. If the drift velocity is low, recombination is favored. While E is limited by the onset of gas multiplication, the best resolution is generally obtained with low gas pressures.

The high voltage applied to the Si-detector tends to break down earlier than if it were operated in a high vacuum or at atmospheric pressure. Especially the pressure range from 10^{-3} to 10 mbar turns out to be critical. The maximum safe voltages vary for different Si-detectors even of the same type. Typical values found in a (90 % Ar + 10 % CH_4) mixture are 300-700 V at 25 mbar, 500-900 V at 65 mbar, and 700-1200 V at 130 mbar.

One of the adjustable parameters of the gas detector is the nature of the gas. Most of the measurements were made with a (90 % Ar + 10 % CH_4) mixture. However, combining higher molecular weight and lower average nuclear charge makes pure isobutane about 2.75 times more

effective than conventional argon-methane at the same pressure /11/.

By setting the gas pressure the range of nuclear charge numbers Z of particles which can be identified is affected too. The Z range subtends normally more than 10 successive Z values. Generally, low pressure of 25-65 mbar is used for the detection of heavier ions, e.g. $Z > 10$. In this case, the energy thresholds, which are caused by stopping the ions before they reach the E detector and also by the special form of the energy-loss curve below the Bragg maximum, are relatively small. On the other hand, a higher pressure, 130-270 mbar, is necessary for detection of light ions, which have smaller ionization powers and, thus, induce smaller ΔE pulses.

The low energy threshold mentioned is closely related to the gas thickness. In Fig. 8, the energy losses are plotted of ions with nuclear charge numbers $Z \leq 10$ in a (90 % Ar + 10 % CH_4) mixture at 0.3 and 1.5 mg/cm^2. For comparison, also energy losses in a 0.1 mg/cm^2 Mylar entrance foil are presented. The energy losses are approximately the same for e.g. a 0.2 mg/cm^2 Ti-target.

The performance of the gas-silicon telescope was examined experimentally by studying the nucleon transfer to the projectile in the course of ^{6}Li bombardment of some medium-heavy targets /12/. A typical spectrum obtained from the (^{6}Li + ^{27}Al) reaction at E_{LAB} = 156 MeV and $\Theta = 20^\circ$ is shown in Fig. 9. The pressure of the argon-methane mixture was 50 mbar, and the operation potentials were 0 V, +130 V, and +400 V for the cathode, the Frisch grid, and the anode, respectively. The electronic configuration for data acquisition

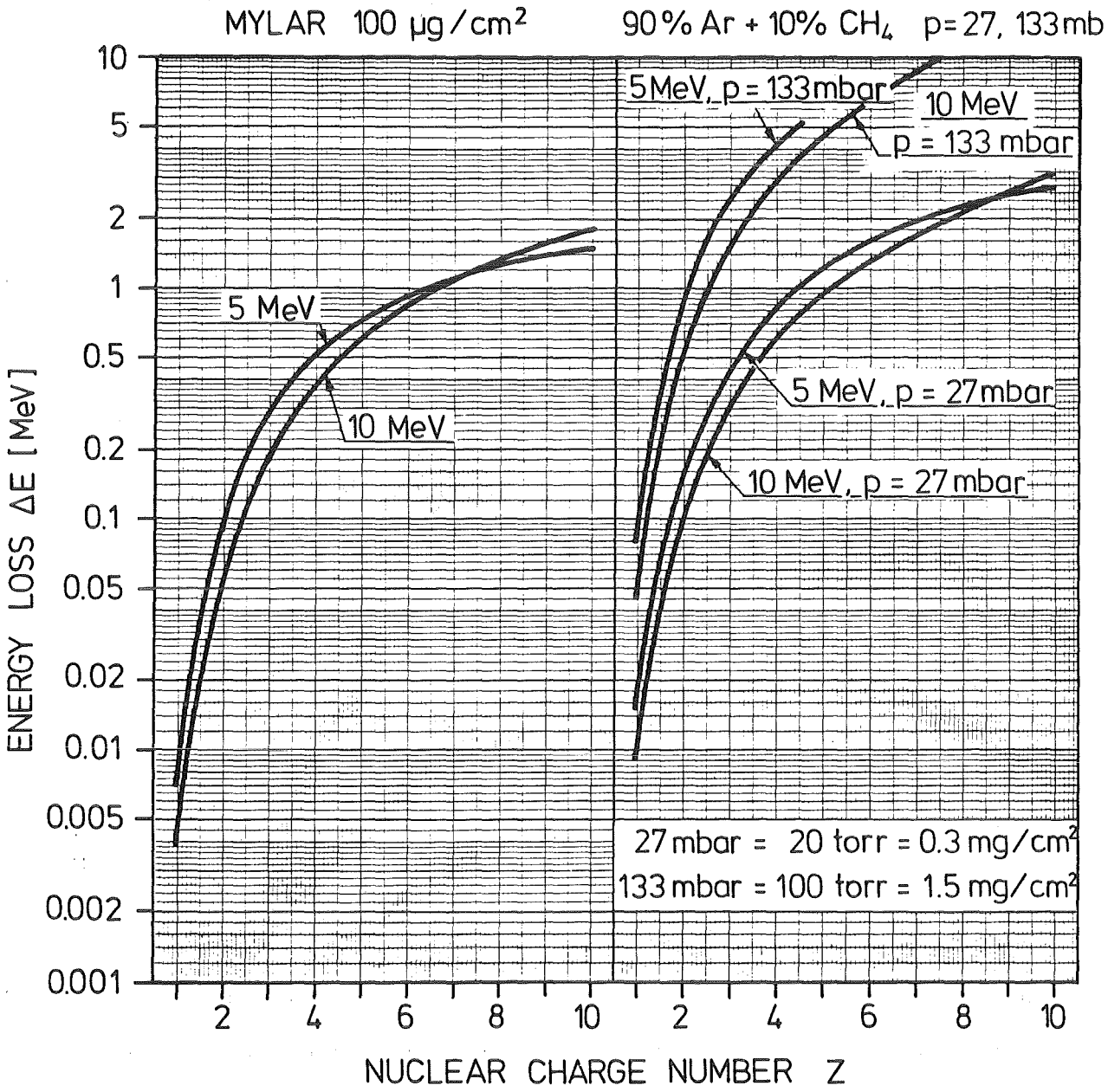

Fig. 8: Energy losses of light and medium-heavy ions as a function of the entrance energy (compiled from Ref. 13).

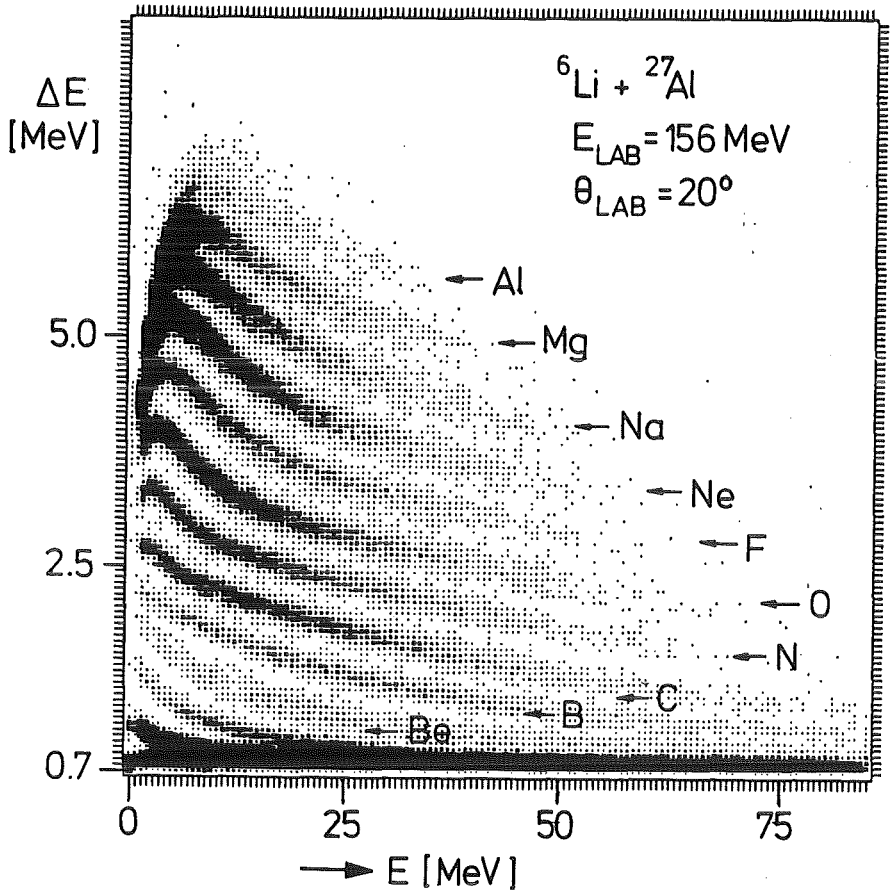

Fig. 9: Typical E-E spectrum

included a slow coincidence unit as shown in the upper part of Fig. 7. The separation of the successive Z products is straightforward above the ΔE maxima. For light products the Z resolution approaches the quality which is necessary for element identification. So its performance compares well with alternative designs reported in literature /5/,/10/.

We acknowledge gratefully the helpful contributions of many persons, especially of Prof. Dr. K. Grotowski, who has placed the Cracow prototype to our disposition, of Mr. W. Albinus and Mr. M. Dürr for careful mechanical elaboration, and of Mr. F. Deutsch, Mr. H.-J. Rimbach and Mr. G. Pätzold for development of the gas control unit.

7. References

/1/ J.B.A. England, "Techniques in Nuclear Structure Physics", The MacMillan Press Ltd., 1974.

/2/ F.S. Goulding and B.G. Harvey, Ann. Rev. Nucl. Sci. **25** (1975) 167.

/3/ F.S. Goulding, Nucl. Instr. Meth. **162** (1979) 609.

/4/ O.R. Frisch, "Isotopic Analysis of Uranium Samples by means of their alpha-ray Groups", BR-49 (1944).

/5/ Jagellonian University Cracow, Department of Electronics, unpublished; see also

J. Brzychczyk, L. Freindl, K. Grotowski, Z. Majka, S. Micek, R. Planeta, M. Albinska, J. Buschmann, H. Klewe-Nebenius, H.J. Gils, H. Rebel, and S. Zagromski, Nucl. Phys. **A417** (1984) 174.

/6/ S. Bohrmann, H. Brösicke, G. Diehl, H. Gemmeke, D. v. Harrach, J. Lauer, A. Richter, G. Ruf, H.J. Specht, in: Jahresbericht, Max Planck Institut für Kernphysik Heidelberg (1974), p. 102, contr. 8.1.6.

/7/ T.E. Cranshaw and J.A. Harvey, N.C.R. Report PD-285 (1946).

T.E. Cranshaw and J.A. Harvey, Can. J. Res. **A26** (1948) 243.

/8/ O. Bunemann, T.E. Cranshaw, J.A. Harvey, Can. J. Res. **A27** (1949) 191.

O. Bunemann, N.C.R. Report PD-285 (1946).

/9/ M. Heinz, Aufbau eines ortsempfindlichen Akzeptanzdetektors für den Magnetspektrograph am Karlsruher Isochron-Zyklotron, Diplomarbeit Karlsruhe University (1984).

/10/ M.M. Fowler and R.C. Jared, Nucl. Instr. Meth. **124** (1975) 341.

/11/ J.R. Erskine, T.H. Braid, J.C. Stoltzfus, Nucl. Instr. Meth. **135** (1976) 67.

J. Barrette, P. Braun-Munzinger, and C.K. Gelbke, Nucl. Instr. Meth. **126** (1975) 181.

/12/ T. Kozik, J. Buschmann, K. Grotowski, H. Klewe-Nebenius, H.J. Gils, H. Jelitto, R. Planeta, H. Rebel, S. Zagromski, in: KfK 3969 (1985), p. 40, contr. 1.3.6.

/13/ L.C. Northcliffe and R.F. Schilling, Nuclear Data Tables **A7** (1970) 233-463.